Supporting Information

Young et al. 10.1073/pnas.1213060110

SI Text

Plasmid Construction. All plasmids were cloned using *Escherichia coli* strain Dh5α and a combination of standard molecular cloning techniques and nonligase-dependent cloning, using Clontech In-Fusion Advantage PCR Cloning kits. Plasmid constructs were integrated into *Bacillus subtilis* chromosomal regions via double crossover, using standard techniques. The following list provides a description of each plasmid constructed, with details on integration position/cassette and selection marker given at the beginning. Note that all plasmids listed below replicate in *E. coli* but not in *B. subtilis*.

Plasmid list.

i) *sacA::P_{sigB}-yfp Cm^R*: The promoter immediately upstream of RsbV, containing a well-characterized σ^B promoter, was cloned into the EcoRI/BamHI sites of AEC127 (1), yielding a Venus (YFP) reporter for σ^B activity.

ii) *amyE::$P_{hyperspank}$-RsbX Spect^R*: The region from 365 bp upstream of RsbX to the end of the RsbX coding region, along with a 5′ transcriptional terminator, was cloned behind the $P_{hyperspank}$ IPTG-inducible promoter in plasmid pDR-111 (gift of D. Rudner, Harvard University, Cambridge, MA).

iii) *amyE::P_{sigb}-3xCFP Spect^R*: This alternative σ^B reporter, containing three tandem copies of the CFP fluorescent protein gene, was used in combination with *yfp* reporters of different genes.

iv) *sacA::P_{opuE}-yfp Cm^R*: The OpuE promoter was cloned into the EcoRI/BamHI sites of AEC127 (1).

B.subtilis strains. Strains used were in the PB2 genetic background, except where noted. Antibiotic resistance was switched using a previously described antibiotic switching vector system (2). Deletions were made by replacing genes of interest with a selection marker via a linear DNA fragment homologous to the region of interest. Many starting strains/genomic DNA were kind gifts of C. W. Price (University of California Davis, CA). Under the construction procedure, the "→" symbol indicates an integration event from plasmid or genomic DNA into the strain after the arrow. For example, in strain JJB839, the construction procedure is listed as "JJB751 → JJB557 (with Neo selection)," meaning "the genomic DNA of JJB751 was prepared and transformed into JJB557 with selection on Neo."

Strain information and construction

	Strain name	Genotype	Construction procedure	Source
1	PB2	*trpC2* (this genotype omitted in derived strains, below)		BGSC 1A776
2	JJB223	P_{spac}-*rsbVWBX* Erm^R; *sacA::P_{sigB}-yfp* Cm^R; *ppsb::P_{trpE}-mCh Phleo^R*		Locke et al. (7)
3	JJB554	amyE::P_{sigB}-*3xCFP; ppsb::P_{trpe}-mCh* Phleo^R		Locke et al. (7)
4	JJB557	JJB554; *rsbQP::*Tet^R		Locke et al. (7)
5	JJB629	*rsbQP::*Tet^R; *sacA::P_{sigB}-yfp* Cm^R; *ppsb::P_{trpe}-mCh* Phleo^R		Locke et al. (7)
6	JJB751	PB2; *ytvA::*Neo^R	Δ*ytvA* Erm^R → PB2. Antibiotic cassette switched from Erm^R to Neo^R	This work
7	JJB761	JJB629; *ytvA::*Neo^R	JJB751 → JJB176 (with Neo^R selection)	This work
8	JJB814	JJB223; *ytvA::*Neo^R; *rsbQP::*Tet^R	*ytvA::*Neo^R → *rsbQP::*Tet^R → JJB223	
9	JJB835	JJB761; $P_{hyperspank}$-*rsbX*	Plasmid (2, from plasmid list) → JJB761	This work
10	JJB837	JJB835; Δ*rsbX* Erm^R;	Erm^R recombination at the *rsbX* locus	This work
11	JJB839	JJB557; *ytvA::*Neo^R	JJB751 → JJB557 (with Neo^R selection)	This work
12	JJB848	JJB839; *sacA::P_{OpuE}-yfp* Cm^R	Plasmid (4, from plasmid list) → JJB839	This work

Microscopy. All data were acquired using a CoolSnap HQ2 attached to a Nikon inverted TI-E microscope, equipped with the Nikon Perfect Focus System (PFS) hardware autofocus module. Molecular Devices commercial software (Metamorph 7.5.6.0) controlled microscope, camera, motorized stage (ASI Instruments), and epifluorescent and brightfield shutters (Sutter Instruments). Epi-illumination was provided by a 300-W Xenon light source (LamdbaLS; Sutter Instruments) connected via a liquid light guide into the illuminator of the scope. Phase contrast illumination was provided by a halogen bulb to allow verification of cell focus and cell shape. Temperature control was achieved using an enclosed microscope chamber (Nikon) attached to a temperature-sensitive heat exchanger set to 37 °C. All experiments used a Phase 100× Plan Apo (NA 1.4) objective. Chroma filter sets used were as follows: 41027 (mCh), 41028 (YFP), and 31044v2 (CFP). The interval between consecutive imaging was 10 min.

Sample Preparation. For agarose movies, samples were prepared using similar protocols to those described in ref. 3 with the following adaptations. For the ethanol experiments showing the environmental PAM response, cells were spotted on Spizizen's minimal media (SMM) agarose pads (without ethanol) and allowed to outgrow for ∼2 h, before the start of imaging. When ethanol was to be added, 4 μL of ethanol solution was added to the top of the agarose pad and then immediately a small, glass-topped cap was placed around each individual pad to prevent ethanol evaporation.

Microfluidics. Cells were grown using the Cellasic ONIX microfluidic perfusion system with a bacterial plate (B04A). Cells

were loaded onto the plate at an approximate OD of 0.001, using the automated Cellasic loading protocol. The settings for loading pressure were between 4 and 6.5 psi, and loading times were between 2 and 4 s. This often loaded cells at a very low density, suitable for time-lapse imaging and quantitative analysis. Cell growth and responses to stress were similar between pad and microfluidic conditions. To create a linear gradient of increasing stress, pressures across the microfluidic manifold were changed in 20 discrete steps from no stress to maximum stress. The appropriate pressures necessary to generate a linear gradient were calibrated from fluorescein dye measurements.

Growth Conditions. SMM is derived from Spizizen's minimal media (4), which uses 0.5% glucose as the carbon source and tryptophan (50 μg/mL) as an amino acid supplement. Ethanol and NaCl were dissolved in SMM and diluted to working concentrations, depending on whether the experiment was in pad or liquid conditions. IPTG was dissolved in H_2O and diluted 1,000-fold into working concentrations.

Ethanol experiments. Cells were grown from glycerol stocks in SMM to midlog (OD = 0.3–0.8) and then diluted back into SMM to an OD of 0.01. After regrowing to OD = 0.1 at 37 °C, cells were then spotted on SMM 1.5% (wt/vol) low-melt agarose pads. After allowing cells to equilibrate after 2–3 h, time-lapse acquisition was started. Ethanol was added to pads as described above.

Rate-responsive measurements. Cells were grown from glycerol stocks in SMM to midlog and then diluted back into SMM to an OD of 0.01. After regrowth to OD = 0.1 at 37 °C, cells were loaded into the microfluidic plate using all four chambers, using the protocol described above. After 2 h of outgrowth, time-lapse imaging was started. For each plate, two chambers were exposed to fast stress, using a step in stress, whereas the other two chambers were exposed to slow stress, using a 20-step gradient as described above. For ethanol experiments, the final ethanol concentration was 2%, whereas for osmotic experiments the final NaCl concentration was 0.4 M.

Dose–response measurements. In the *rsbX* feedback-independent strain (JJB837), the expression of rsbX is controlled by the amount of IPTG in the culture. The absence of rsbX results in uncontrolled activation of σ^B, which strongly reduces cell growth rate. To maintain minimal σ^B activity, JJB837 was grown from glycerol stocks with 1mM IPTG to midlog. Cells were then washed with several exchanges of SMM without IPTG, and the resulting culture was diluted to OD = 0.01 with varying levels of IPTG (10, 30, 100, and 1,000 μM). Upon regrowth to OD = 0.1 in SMM, culture volume was split and ethanol was added to varying final concentrations (0, 0.5, 1, 1.5, 2, 2.5, 3, 3.5, and 4%). After 30 min of ethanol exposure, cells were spotted on PBS 1.5% agarose pads and imaged. The time between spotting of pads and imaging was kept to a minimum, with the entire process taking 15–20 min for each sample. Consistent with this principle, the dose–response curves for each strain/IPTG concentration were measured independently of each other to minimize sample preparation times for each sample. Snapshots were analyzed using custom MATLAB software.

RNAseq. ***Growth conditions.*** Cells were grown overnight as described above to midlog. Cells were diluted back to OD = 0.001 into three conditions (fast stress, slow stress, and no stress) with two replicates and allowed to grow at 37 °C for 1 h. Diluting cells to a very low concentration allowed the experiment to proceed without entering stationary phase.

NaCl RNAseq. In the slow-stress conditions, 10 μL of a 4-M NaCl solution was added to 2 mL of culture every 20 min for 20 steps (400-min ramp), to closely mimic the microfluidic experiments. Upon the addition of the last step, 200 μL of the same NaCl solution was added to the fast-stress conditions to yield the same final salt concentration (0.36 M NaCl). After 10 min of additional growth at 37 °C, samples were then prepared for RNA extraction. Two hundred microliters of culture continued to grow, and snapshots of the cells were taken 30 min after the last addition of NaCl.

Ethanol RNAseq. The experiment was performed as in the NaCl experiment, except that ethanol was used in place of NaCl. The final concentration of 1% ethanol induced similar peak σ^B activation compared with 0.36 M NaCl when added to cells immediately.

Library preparation. RNA from ∼2 mL of culture was extracted using the Qiagen RNeasy Protect Bacteria Mini Kit (74524), using 5 mg/mL lysozyme for cell lysis. Ten nanograms of RNA was used subsequently for RNAseq library creation, using the Epicentre ScriptSeq v2 RNA-Seq Library Preparation Kit (SSV21106). Using this kit requires additional materials as described in the protocol. For the cDNA purification step, the Qiagen MinElute PCR Purification kit was used, and for the final library purification, the Agencourt AMPure XP System (Beckman Coulter) was used. Each sample was uniquely labeled with Epicentre's ScriptSeq Index PCR Primers. The completed libraries were submitted to the California Institute of Technology (Caltech) Sequencing Core facility. Libraries were sequenced with 50-bp reads, using the standard Solexa (Illumina) protocol and pipeline.

Data analysis. Illumina raw data provided by the GERALD (Illumina) software package were aligned to a FASTA file containing the *B. subtilis* genome, using the Maq short read aligning program (Wellcome Trust Sanger Institute, Hinxton, UK). Maq-aligned reads were converted into a .BAR file, using the Cisgenome software (Stanford University, Stanford, CA) (5). Total reads for each gene and further calculations were performed using MATLAB and DESeq.

Quantitative Analysis. Quantitative movie analysis used custom image analysis code in MATLAB, described in ref. 6. Calculation of single-cell promoter activity is similar to that described in ref. 7.

Colony promoter activity is defined as the amount of protein produced per unit colony area. Unlike in single cells, here the relative impact of potential segmentation errors is strongly reduced by averaging over the entire colony. We define colony promoter activity as

$$P_{colony} = \frac{1}{A(t)}\frac{dF_{tot}(t)}{dt} + \gamma\frac{F_{tot}(t)}{A(t)}.$$

Here, $A(t)$ represents total colony area in pixels, and F_{tot} is integrated fluorescence over the entire colony. To avoid unphysical negative values of promoter activity due to bleaching of fluorescent proteins during the movie, we set the photobleaching rate $\gamma = 0.05$ for all movies analyzed in this work.

Minimal Model of σ^B Network. To model activation of σ^B by the environmental stress pathway we modified our model of σ^B activation by energy stress (7). This model is extremely simplified, concentrating on the minimal components necessary to explain σ^B pulse generation. It does not model in detail the dynamics of the network. The model is described below.

Here we combine the functions of RsbV and σ^B into a generalized activator, denoted A. Like RsbV, A is active in its unphosphorylated form and inactive when phosphorylated (A_P). A phosphatase, functionally analogous to RsbQP and RsbTU complexes, is denoted P. An RsbW-like kinase, K, phosphor-

ylates A. A activates itself and its inhibitor, K via a transcriptional autoregulatory feedback loop.

We assume Michaelis–Menten kinetics for the phosphorylation and dephosphorylation reactions. We also assume linear degradation and transcription rates. These assumptions result in the following continuous ordinary differential equations for the network,

$$\frac{dA}{dt} = trans - phos + dephos - k_d A \quad \textbf{[S1]}$$

$$\frac{dA_P}{dt} = phos - dephos - k_d A_P \quad \textbf{[S2]}$$

$$\frac{dK}{dt} = trans - k_d K, \quad \textbf{[S3]}$$

where

$trans = t_a A + t_i$ is the transcription rate for both A and K, **[S4]**

$dephos = \frac{b_{dp} P A_P}{k_{dp} + A_P}$ is the rate of dephosphorylation, **[S5]**

and

$phos = \frac{b_p K A}{k_p + A}$ is the rate of phosphorylation of A. **[S6]**

Parameter values

Parameter	Description	Value
t_i	Basal transcription rate	0.005 μM/min
t_a	Autoregulatory (induced) transcription rate due to A feedback	0.025 min^{-1}
k_{dp}	A_P concentration (Michaelis constant) for half-maximal dephosphorylation	0.1 μM
k_p	A concentration (Michaelis constant) for half-maximal phosphorylation	0.1 μM
k_d	Degradation rate	0.005 min^{-1}
b_p	Rate constant for phosphorylation	0.065 min^{-1}
b_{dp}	Rate constant for dephosphorylation	0.125 min^{-1}

The equations and parameters above are identical to those used in our previously published energy stress model (7). The sole difference between the energy and environmental stress models is how we treat the phosphatase levels, P. Previously, to model stress activation through the energy stress pathway, we replaced the constant phosphatase level, P, with a time-varying phosphatase concentration, $P(t)$. $P(t)$ was precomputed through a gamma-distributed Ornstein–Uhlenbeck process (7). To model stress activation in the environmental stress pathway, changes in stress are assumed to determine phosphatase levels with negligible delays. This represents the fast release of RsbT by the stressosome. Hence phosphatase levels, P are proportional to stress level (Fig. 2*B*).

1. Eldar A, et al. (2009) Partial penetrance facilitates developmental evolution in bacteria. *Nature* 460(7254):510–514.
2. Steinmetz M, Richter R (1994) Plasmids designed to alter the antibiotic resistance expressed by insertion mutations in Bacillus subtilis, through in vivo recombination. *Gene* 142(1):79–83.
3. Young JW, et al. (2012) Measuring single-cell gene expression dynamics in bacteria using fluorescence time-lapse microscopy. *Nat Protoc* 7(1):80–88.
4. Spizizen J (1958) Transformation of biochemically deficient strains of Bacillus subtilis by deoxyribonucleate. *Proc Natl Acad Sci USA* 44(10):1072–1078.
5. Ji H, et al. (2008) An integrated software system for analyzing ChIP-chip and ChIP-seq data. *Nat Biotechnol* 26(11):1293–1300.
6. Rosenfeld N, Young JW, Alon U, Swain PS, Elowitz MB (2005) Gene regulation at the single-cell level. *Science* 307(5717):1962–1965.
7. Locke JC, Young JW, Fontes M, Hernández Jiménez MJ, Elowitz MB (2011) Stochastic pulse regulation in bacterial stress response. *Science* 334(6054):366–369.

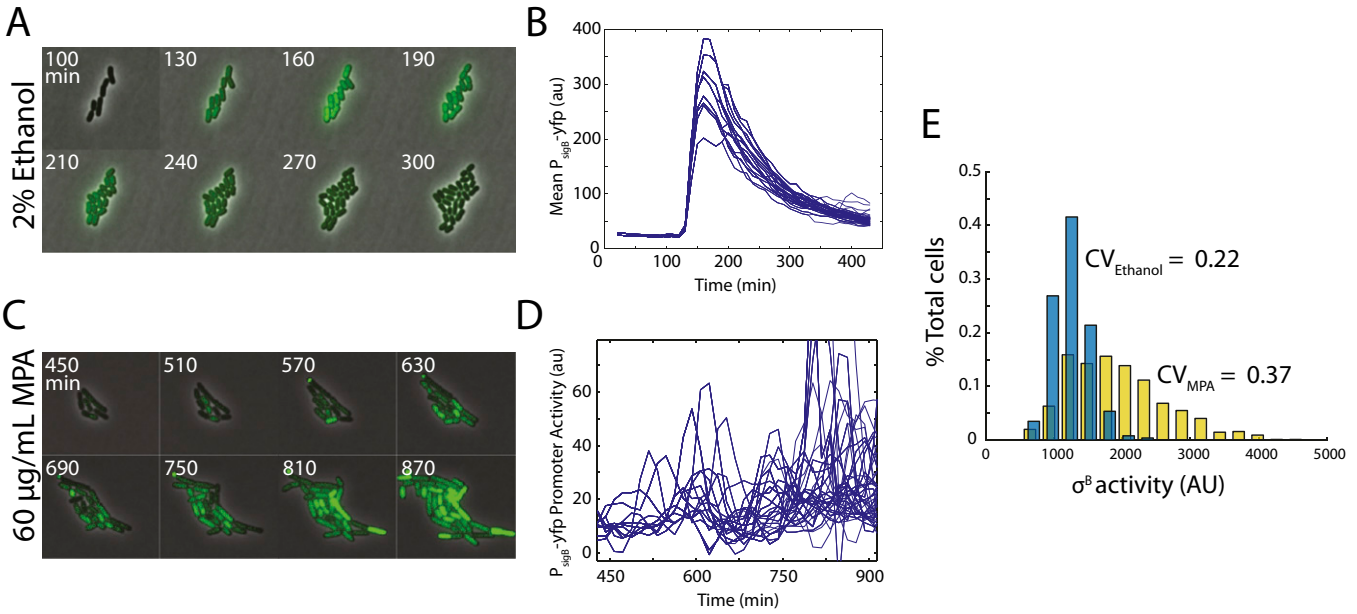

Fig. S1. Environmental stress produces homogeneous pulses of σ^B activation. (*A* and *B*) Filmstrip of P_{sigB}-yfp activation (green) in strain JJB761 in response to a step from 0 to 2% ethanol (reproduced from Fig. 1*B*) (*A*). Note the single pulse of activation in all lineages (*B*). This homogeneity contrasts with σ^B activity under energy stress. (*C* and *D*) Single-lineage traces of strain JJB240 exposed to 60 μM MPA (energy stress) (*C*) show sustained stochastic pulses (*D*). (*E*) In a strain where both energy and environmental sensors are present (JJB213), snapshots of cells cultured in liquid media reveal more variation when exposed to 60 μg/mL MPA (yellow) compared with 2% ethanol (blue), at similar induction levels.

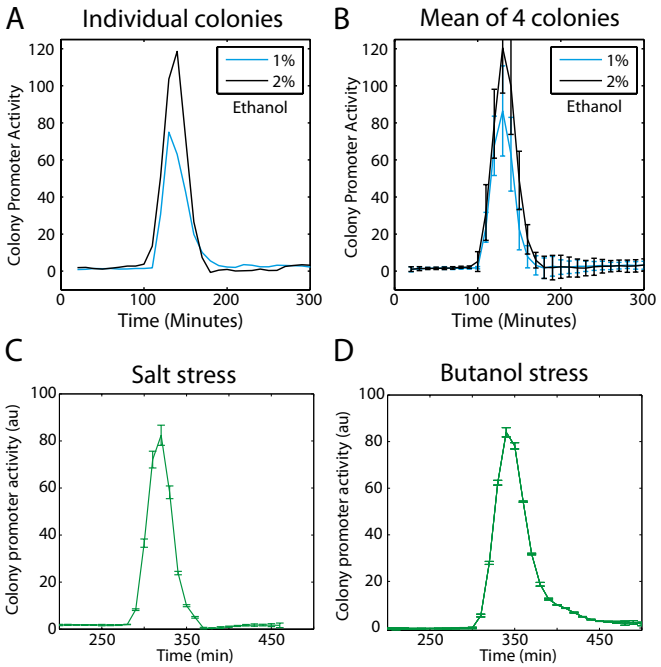

Fig. S2. σ^B responds to ethanol and other environmental stresses with a single adaptive pulse of activity. Extended traces from Fig. 1 show no additional pulsing activity after the single pulse. For clarity, only 1 and 2% ethanol exposure is shown. *A* shows a typical single-colony trace and *B* shows the mean response of four colonies. When grown under microfluidic conditions and exposed to either 0.4 M NaCl (*C*) or 0.25% butanol (*D*), strain JJB761 exhibits a single pulse of activity as measured from a P_{sigB}-yfp promoter reporter. Error bars represent SD of the response across averaged movies.

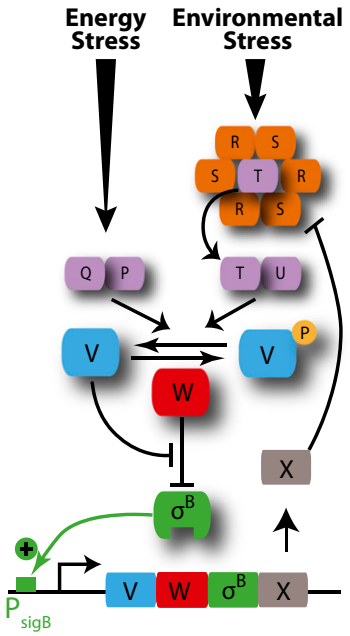

Fig. S3. σ^B regulatory circuit uses distinct input pathways to transduce energy and environmental stresses (schematic). Energy stress causes the phosphatase complex RsbQP (labeled QP) to dephosphorylate RsbV (V) directly. Environmental stress is tranduced by the stressosome, composed of RsbR (R) and RsbS (S) subunits (orange), which controls the availability of RsbT (T, purple), the coactivator of RsbU (U, purple). Active RsbU dephosphorylates RsbV (V, blue). Dephosphorylated RsbV can bind RsbW (W, red), releasing σ^B (green) to activate diverse target genes, including its own operon, as indicated. Activation of the σ^B operon increases expression of the stressosome-specific phosphatase RsbX (X, gray). RsbX acts upon the stressosome to inhibit release of RsbT.

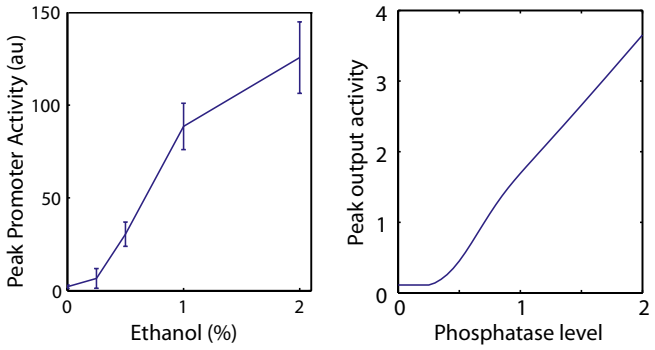

Fig. S4. The stress response curve is approximated by models of phosphatase release. Model parameters predict a relationship between phosphatase level and peak output activity that is in good agreement with experimental results. (*Left*) Ethanol response data (as seen in Fig. 1). (*Right*) Predicted peak σ^B activity as a function of immediate phosphatase release.

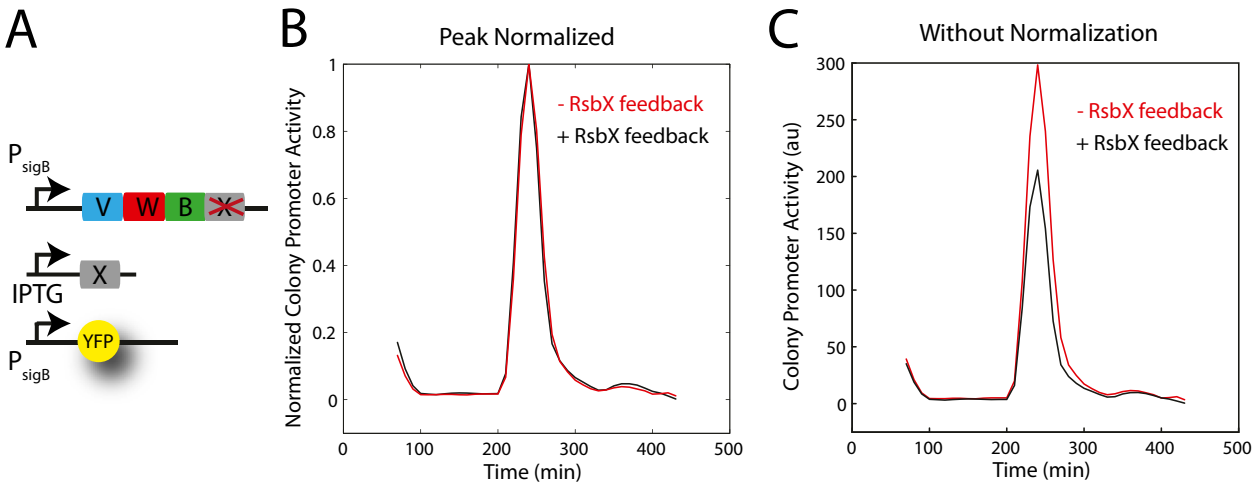

Fig. S5. RsbX feedback is not necessary for adaptive response to environmental stress. (*A*) The wild-type *rsbX* gene was deleted and replaced with an IPTG-inducible copy ($P_{hyperspank}$-rsbX) to create a RsbX feedback-independent strain (−RsbX feedback). This strain required constitutive induction of RsbX to supress σ^B activity. (*B*) Strains with (JJB761) and without (JJB836) feedback were compared in SMM with 1 mM IPTG for the −RsbX feedback strain in a CellASIC microfluidic system. At $t = 200$ min, 2% ethanol was added and P_{sigB}-yfp activity was measured. (*C*) When comparing peak normalized colony promoter activity, the feedback-independent strain exhibits nearly identical dynamics compared with those of the +RsbX feedback strain, but does show differences in peak amplitude.

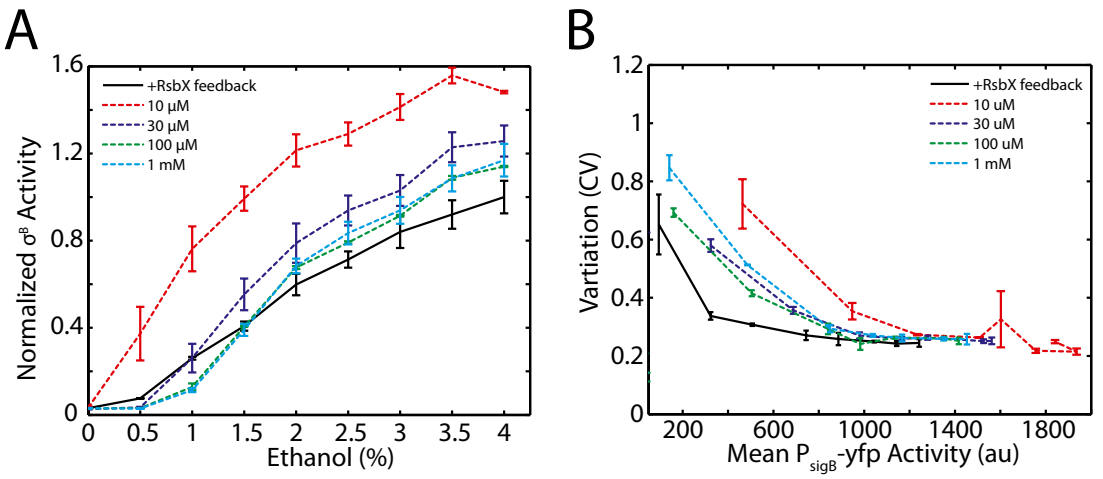

Fig. S6. RsbX feedback linearizes σ^B dose–response curve and reduces expression noise. Strains with (JJB761) or without (JJB836) RsbX-mediated feedback were grown in SMM and exposed to different concentrations of ethanol (0–4%) at indicated IPTG concentrations (for the no feedback strain). Near the peak of activation (30 min of exposure), σ^B activity was measured using a P_{sigB}-yfp reporter via microscope snapshots. (*A*) Negative feedback linearizes the σ^B dose–response curve. Across concentrations of IPTG that give comparable activation (30–1,000 μM) to that of the +feedback strain, the dose–response curve is more nonlinear (compare blue, dark blue, and green to black lines), where responses to low and high levels of ethanol are suppressed and elevated, respectively, compared with those of the +feedback strain. (*B*) P_{sigB}-yfp expression noise is elevated in the −RsbX feedback strain (JJB836). Strains were grown in SMM, either without IPTG (JJB761, +RsbX feedback) or with indicated concentrations of IPTG (JJB836, −RsbX feedback), and were exposed to different concentrations of ethanol (0–4%). Near the peak of activation (30 min of exposure) σ^B activity was measured in static snapshots. At nearly all levels of σ^B activation, the presence of the RsbX feedback loop reduces noise, as measured by the coefficient of variation (CV = SD/mean), compared with the feedback-independent strain.

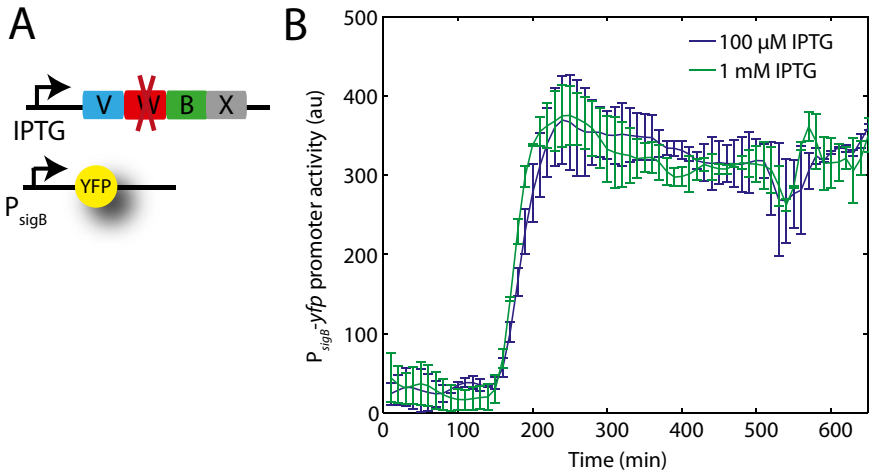

Fig. S7. RsbW is required for termination of σ^B activity. (*A*) The endogenous σ^B operon was replaced by an inducible σ^B operon lacking rsbW. (*B*) This strain exhibited sustained activation of σ^B when induced (t = 170 min) with indicated IPTG concentrations, abolishing the normal adaptive pulse seen with the wild-type strain.

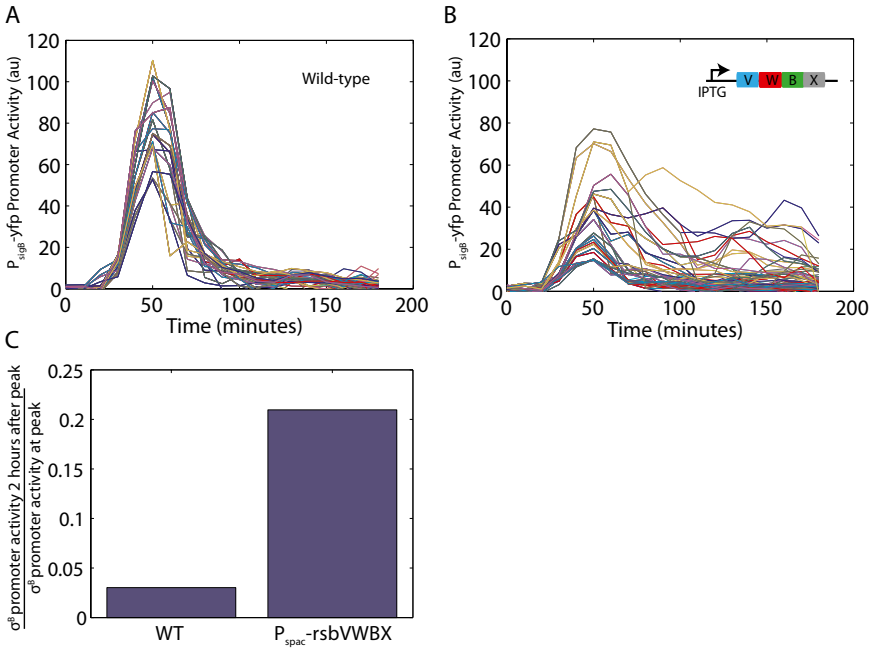

Fig. S8. Feedback loops are required for full adaptation. Reporter cells were stimulated with a step from 0 to 2% ethanol. (*A*) Standard response is a single adaptive pulse. (*B*) In a strain where all feedback loops are removed, and the σ^B operon is under the control of an inducible promoter (induced with 30 μM IPTG) (P_{spac}-rsbVWBX), adaptation after exposure to 2% ethanol is reduced. In both *A* and *B*, traces are from individual cell lineages. (*C*) Comparison of decline in promoter activity 2 h after peak for wild-type and P_{spac}-rsbVWBX strains.

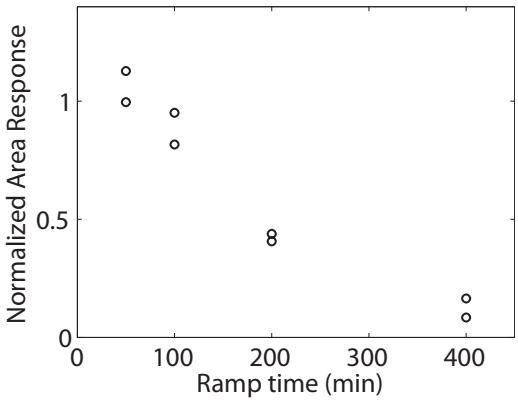

Fig. S9. Other measures of σ^B activation also show rate responsiveness. Integrated promoter activity, where nonnegative promoter activity is summed across the experiment, shows similar rate responsiveness compared with peak amplitude measurements (Fig. 3). Each point reflects the integrated promoter activity for indicated ramp time from 0 to 2% ethanol, normalized to the integrated promoter activity of a step change in ethanol. Duplicate data points come from experiments performed on different days. The data plotted here originate from the same dataset as that in Fig. 3.

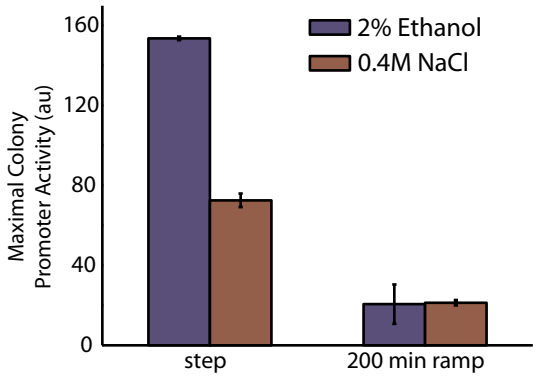

Fig. S10. NaCl activates σ^B in a rate-responsive fashion. Reporter strain JJB761 was exposed to either a step increase or a 200-min ramp to either 2% ethanol or 0.4 M NaCl. Error bars represent SD across 2 d of experiments.

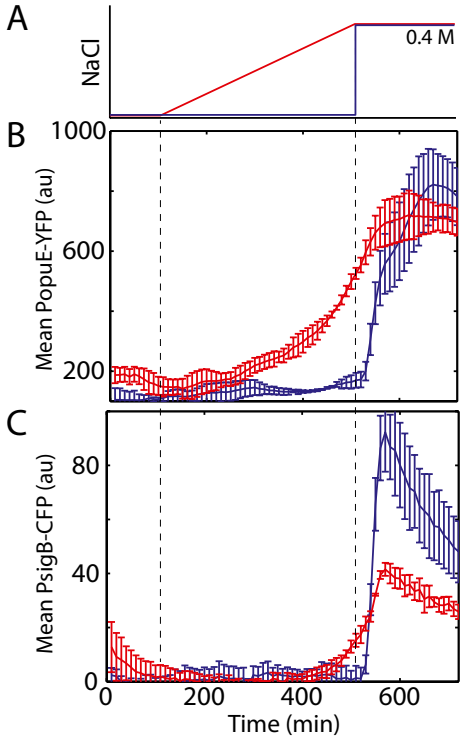

Fig. S11. OpuE shows rate-independent steady-state expression. Strain JJB848 contains P_{opuE}-yfp and P_{sigB}-cfp reporter genes. (*A*–*C*) When exposed to step or 400-min ramps of salt stress (from 0 to 0.4 M) (*A*), mean P_{opuE} promoter activity (*B*) reaches similar steady-state levels compared with P_{sigB} promoter activity in the same strain, shown in *C*. Error bars represent SD for each condition and time point.

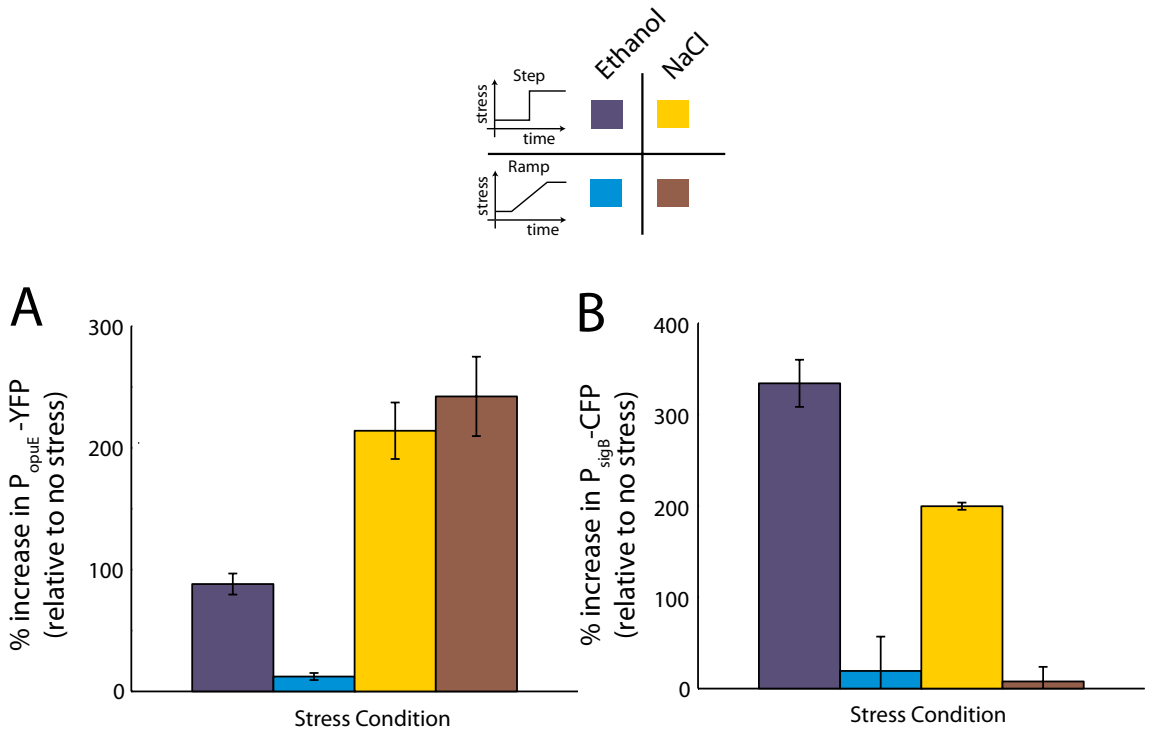

Fig. S12. OpuE is rate responsive to ethanol stress, but not to salt stress. Cells were grown in liquid SMM and exposed to either a step (dark blue) or a 400-min ramp (light blue) of 2% ethanol or a step (yellow) or a 400-min ramp (brown) of 0.36 M NaCl. (*A* and *B*) Snapshots of mean P_{opuE}-yfp (*A*) and P_{sigB}-cfp (*B*) were taken 30 min after the end of stress application. Error bars are SD.

Table S1. σ^B independent, multiregulated, and exclusive stress-induced genes

σ^B-independent response genes	Inducing stresses	σ^B multiregulated genes*	Listed regulators*	Exclusive σ^B targets*
dnaK	Heat (1)	Bmr	sigB, sigA, BmrR, Mta	csbC
groE	Heat (2)	ctsR	sigB, sigA, ctsR	csbD
proHJ	Osmotic	gtaB	sigB, sigA	csbX
narG	Anaerobic (3)	nadE	sigA, sigB	ctc
lctE	Anaerobic (3)	opuE	sigB, sigA	dps
dhb	Iron limitation (4)	trxA	sigB, sigA	gsiB
mrgA	Oxidative	yfhL	sigB, sigW	gspA
comK	Nutrient limitation	yfkH	sigB, sigA	nhaX
tagC	DNA damage	yhdN	sigB, ylpC	yacL
Spo0A	Nutrient limitation	yjbC	sigB, ylpC	ydaD
sigM	Ethanol, antibiotics, heat (5)	yjbC	sigB, sigW, sigX	ydaP
		yqhP	sigB, sigF	ydaT
		yqxL	sigB, lexA	yfhK
		ytxG	sigB, sigH	yflA
		yvyD	sigB, sigA, spo0A	yjgB
				ykgA
				yoaA
				ypuC
				yrvD
				ytkL
				yvgO
				yvrE
				ywjC
				ywtG
				yxkO
				yycD
				yacM
				ydaF
				ysnF
				ywmE

*The promoters of 196 genes defining the σ^B regulon from ref. 6 were analyzed for known regulators, using DBTBS (7), and classified as having an exclusive σ^B-dependent promoter, mixed dependence, or other (not shown).

1. Wetzstein M, et al. (1992) Cloning, sequencing, and molecular analysis of the dnaK locus from Bacillus subtilis. *J Bacteriol* 174(10):3300–3310.
2. Schmidt A, Schiesswohl M, Völker U, Hecker M, Schumann W (1992) Cloning, sequencing, mapping, and transcriptional analysis of the groESL operon from Bacillus subtilis. *J Bacteriol* 174(12):3993–3999.
3. Ye RW, et al. (2000) Global gene expression profiles of Bacillus subtilis grown under anaerobic conditions. *J Bacteriol* 182(16):4458–4465.
4. Bsat N, Helmann JD (1999) Interaction of Bacillus subtilis Fur (ferric uptake repressor) with the dhb operator in vitro and in vivo. *J Bacteriol* 181(14):4299–4307.
5. Thackray PD, Moir A (2003) SigM, an extracytoplasmic function sigma factor of Bacillus subtilis, is activated in response to cell wall antibiotics, ethanol, heat, acid, and superoxide stress. *J Bacteriol* 185(12):3491–3498.
6. Nannapaneni P, et al. (2012) Defining the structure of the general stress regulon of Bacillus subtilis using targeted microarray analysis and random forest classification. *Microbiology* 158(Pt 3):696–707.
7. Sierro N, Makita Y, de Hoon M, Nakai K (2008) DBTBS: A database of transcriptional regulation in Bacillus subtilis containing upstream intergenic conservation information. *Nucleic Acids Res* 36(Database issue):D93–D96.

Table S2. Genes up-regulated under fast step stress conditions but not identified as σ^B targets (ref. 1)

Gene	Fold up-regulated: fast step	Fold up-regulated: slow ramp	Sensitivity ratio*
Etoh stress			
KatX(yxlI)	90.6	2.2	41.1
ydaH	9.3	1.7	5.4
yumB	8.1	0.8	9.7
yhcW	7.8	1.1	7.2
yhcX	7.1	1.2	5.9
yhdX	6.3	1.1	5.7
Salt stress			
KatX(yxlI)	154.7	11.8	13.1
yyzH	50.3	7.0	7.2
yrkA	35.3	11.1	3.1
ykrP	39.1	2.8	14.0
ykzN	24.7	5.7	4.3
mntD	21.9	2.2	10.0
mntC	17.6	1.8	9.8
yjoB	13	1.0	13.4

*Sensitivity ratio: fast step expression/slow ramp expression.

1. Nannapaneni P, et al. (2012) Defining the structure of the general stress regulon of Bacillus subtilis, using targeted microarray analysis and random forest classification. *Microbiology* 158(Pt 3):696–707.

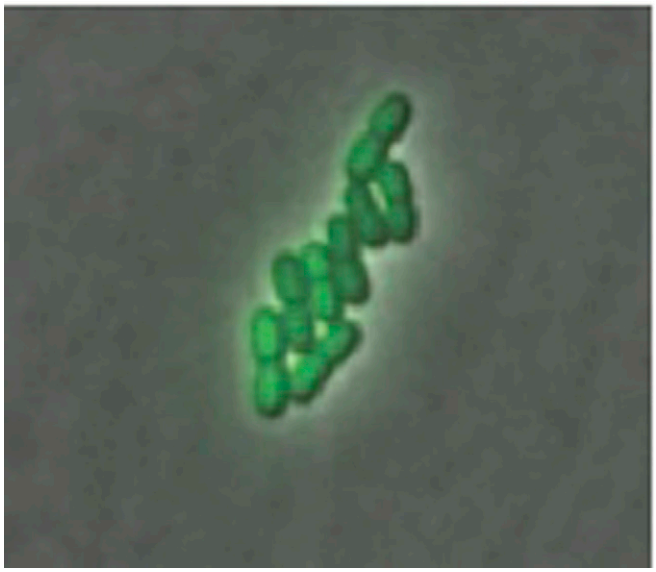

Movie S1. Time-lapse movie of cells containing a P_{sigB}-yfp reporter exposed to 2% ethanol, a type of environmental stress, on a SMM agarose pad. The fluorescence channel is colored in green, and combined with the phase image to produce a composite. The time between consecutive frames is 10 min. Mean cell fluorescence is plotted in Fig. S1*B*.

Movie S1